Supplemental data

Title: Color modulation by selective excitation activated defects and complex cation distribution in $Zn_{1-x}Mg_xAl_2O_4$ nanocrystals

Megha Jain, Manju, Manish Kumar, Hyun Hwi Lee, Sung Ok Won, Keun Hwa Chae, Ankush Vij, and Anup Thakur**

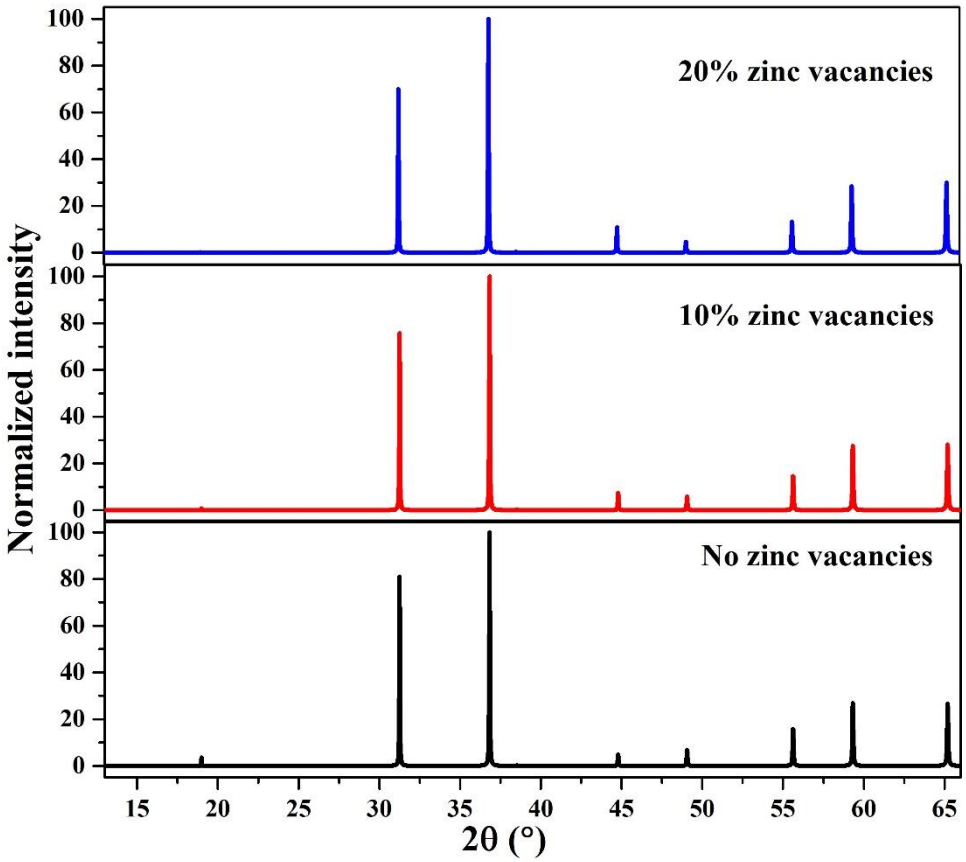

Figure S1. Simulated XRD patterns of $ZnAl_2O_4$ with no zinc vacancy, 10% and 20% zinc vacancies.

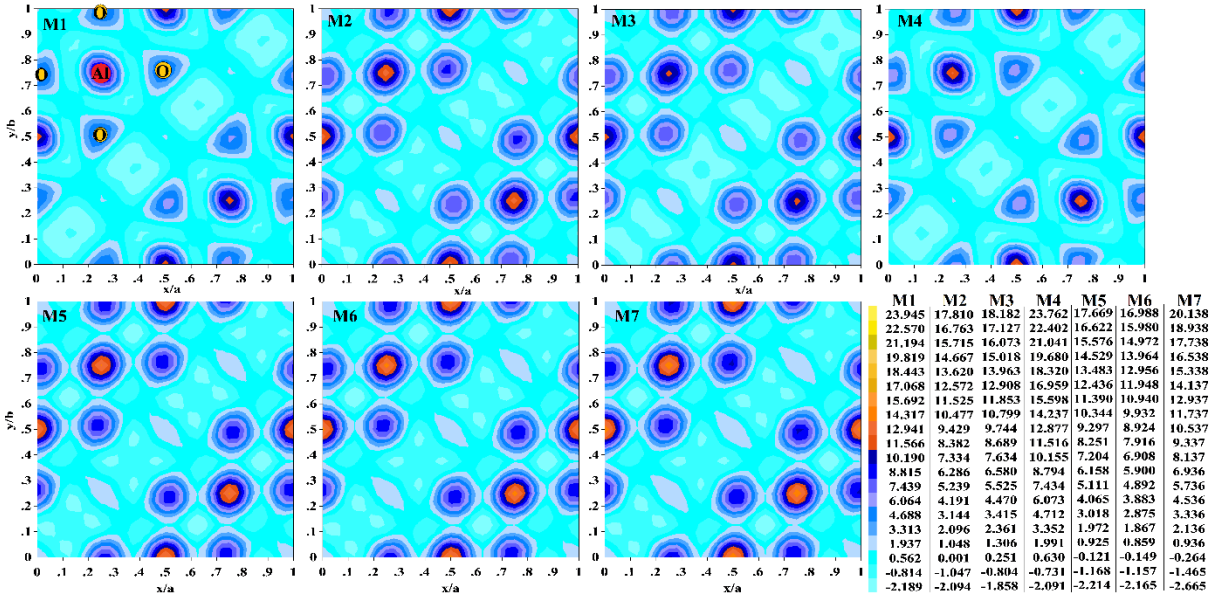

M1	M2	M3	M4	M5	M6	M7
23.945	17.810	18.182	23.762	17.669	16.988	20.138
22.570	16.763	17.127	22.402	16.622	15.980	18.938
21.194	15.715	16.073	21.041	15.576	14.972	17.738
19.819	14.667	15.018	19.680	14.529	13.964	16.538
18.443	13.620	13.963	18.320	13.483	12.956	15.338
17.068	12.572	12.908	16.959	12.436	11.948	14.137
15.692	11.525	11.853	15.598	11.390	10.940	12.937
14.317	10.477	10.799	14.237	10.344	9.932	11.737
12.941	9.429	9.744	12.877	9.297	8.924	10.537
11.566	8.382	8.689	11.516	8.251	7.916	9.337
10.190	7.334	7.634	10.155	7.204	6.908	8.137
8.815	6.286	6.580	8.794	6.158	5.900	6.936
7.439	5.239	5.525	7.434	5.111	4.892	5.736
6.064	4.191	4.470	6.073	4.065	3.883	4.536
4.688	3.144	3.415	4.712	3.018	2.875	3.336
3.313	2.096	2.361	3.352	1.972	1.867	2.136
1.937	1.048	1.306	1.991	0.925	0.859	0.936
0.562	0.001	0.251	0.630	-0.121	-0.149	-0.264
-0.814	-1.047	-0.804	-0.731	-1.168	-1.157	-1.465
-2.189	-2.094	-1.858	-2.091	-2.214	-2.165	-2.665

Figure S2. Observed Fourier electron density maps of all samples in the direction [001] of cubic unit cell for layer containing Al bonded to oxygen atoms (origin is considered at $\bar{3}m$ on the octahedral vacancy).

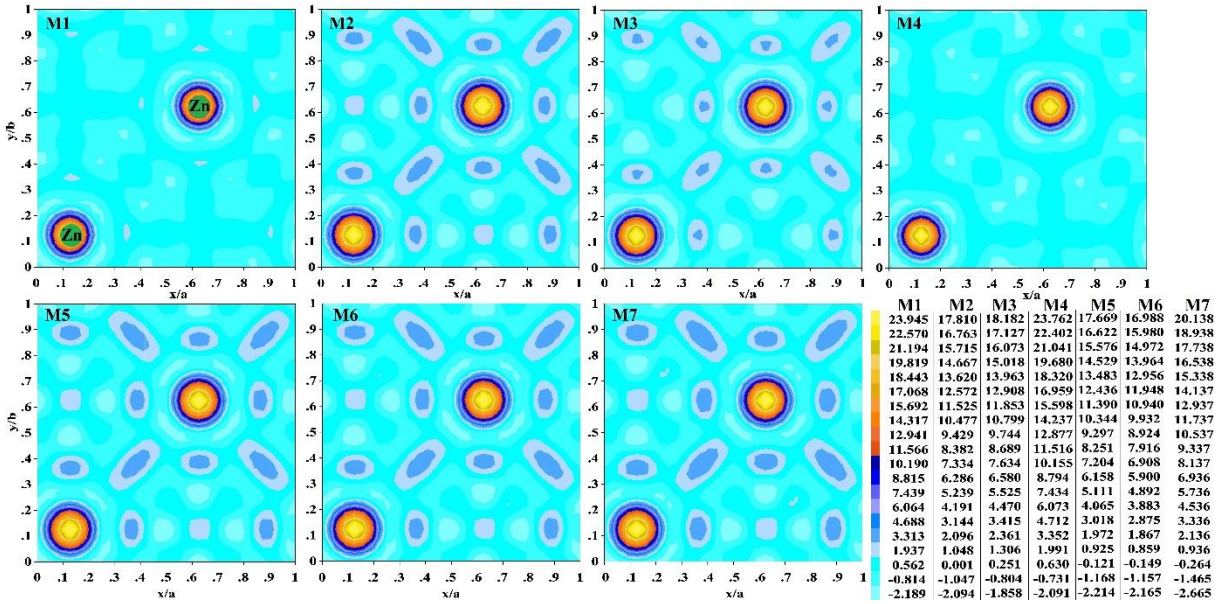

M1	M2	M3	M4	M5	M6	M7
23.945	17.810	18.182	23.762	17.669	16.988	20.138
22.570	16.763	17.127	22.402	16.622	15.980	18.938
21.194	15.715	16.073	21.041	15.576	14.972	17.738
19.819	14.667	15.018	19.680	14.529	13.964	16.538
18.443	13.620	13.963	18.320	13.483	12.956	15.338
17.068	12.572	12.908	16.959	12.436	11.948	14.137
15.692	11.525	11.853	15.598	11.390	10.940	12.937
14.317	10.477	10.799	14.237	10.344	9.932	11.737
12.941	9.429	9.744	12.877	9.297	8.924	10.537
11.566	8.382	8.689	11.516	8.251	7.916	9.337
10.190	7.334	7.634	10.155	7.204	6.908	8.137
8.815	6.286	6.580	8.794	6.158	5.900	6.936
7.439	5.239	5.525	7.434	5.111	4.892	5.736
6.064	4.191	4.470	6.073	4.065	3.883	4.536
4.688	3.144	3.415	4.712	3.018	2.875	3.336
3.313	2.096	2.361	3.352	1.972	1.867	2.136
1.937	1.048	1.306	1.991	0.925	0.859	0.936
0.562	0.001	0.251	0.630	-0.121	-0.149	-0.264
-0.814	-1.047	-0.804	-0.731	-1.168	-1.157	-1.465
-2.189	-2.094	-1.858	-2.091	-2.214	-2.165	-2.665

Figure S3. Observed Fourier electron density maps of all samples in the direction [001] for layer containing Zn atoms (at a height of a/8 of unit cell from first layer in figure S2) (origin is considered at $\bar{3}m$ on the octahedral vacancy).

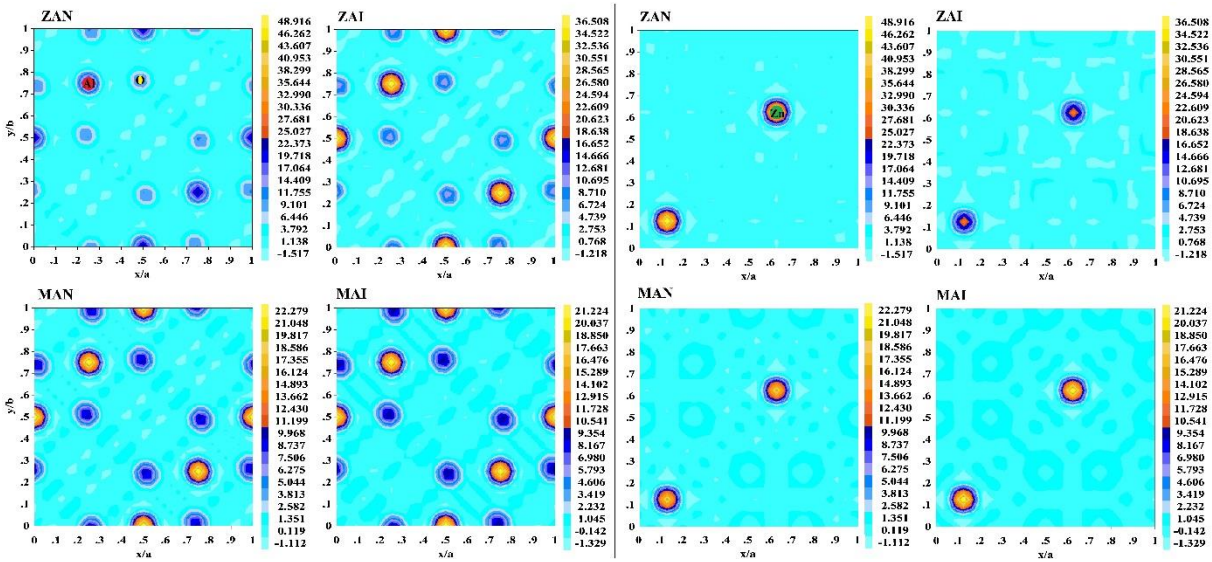

Figure S4. Simulated Fourier electron density maps of zinc aluminate (ZA) and magnesium aluminate (MA) in normal (N) and inverse (I) spinel structure along [001] direction. Density maps on the left correspond to the first layer and those on right are the layers at a height of a/8 from corresponding maps on left.

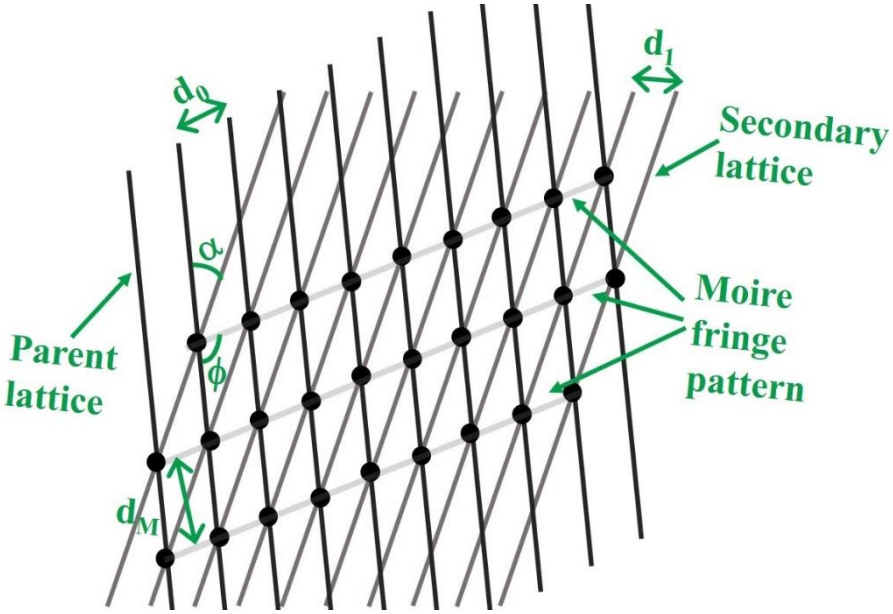

Figure S5. Illustration of Moire fringe pattern formation.

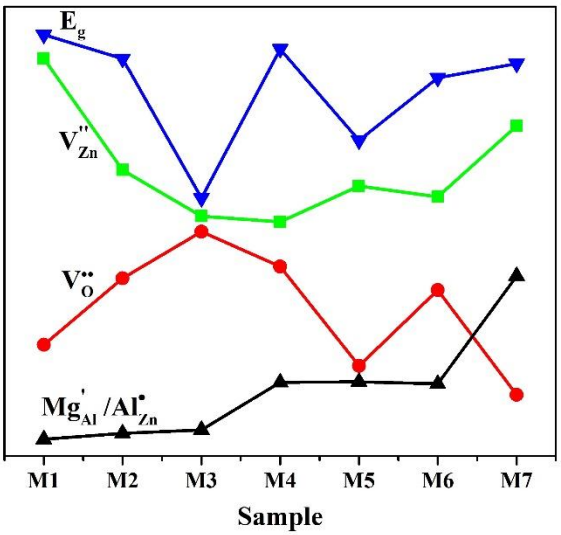

Sample/ doping concentration	V''_{Zn} (%)	$V^{\bullet\bullet}_{O}$(%)	$Mg'_{Al}/Al^{\bullet}_{Zn}$ (%)	E_g (eV)
M1/ (1 %)	5.25	1.50	1.6	4.91
M2/ (5 %)	2.95	2.07	2.5	4.86
M3/ (10 %)	2.00	2.47	3.0	4.57
M4/ (15 %)	1.88	2.17	10.0	4.88
M5/ (20 %)	2.62	1.32	10.1	4.69
M6/ (25 %)	2.40	1.97	9.8	4.82
M7/ (30 %)	3.86	1.07	25.7	4.85

Figure S6. Relative comparison of various defects generated in $Zn_{1-x}Mg_xAl_2O_4$ samples with Mg addition and change in value of band gap. Table on the right shows the concentration of various defects calculated through Rietveld refinement, and band gap energy values for all samples.

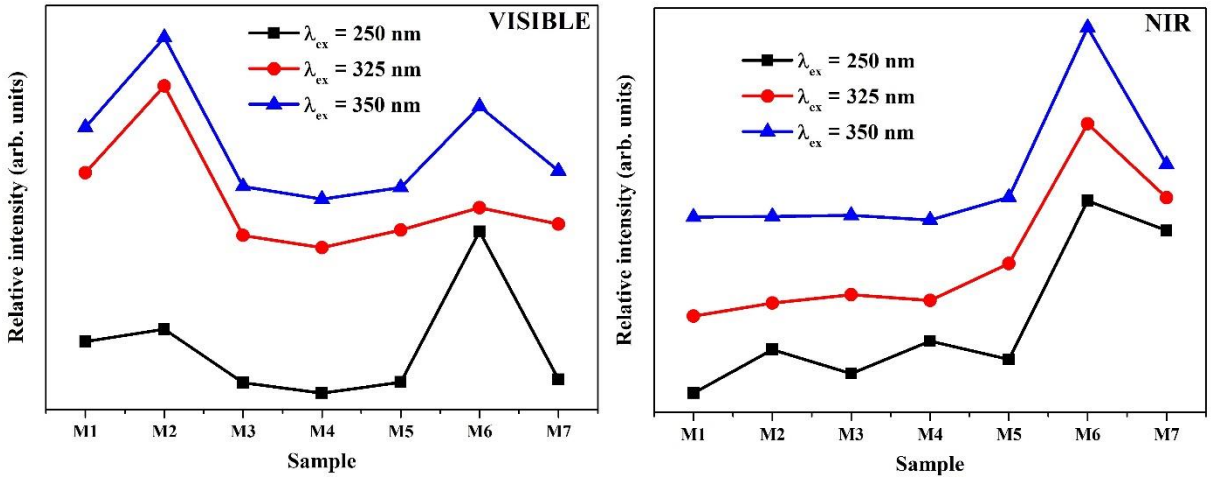

Figure S7. Trend of (a) band I and (b) band II emission integrated intensity of samples.